Raman scattering study of $NaAl(MoO_4)_2$ crystal under high pressures

2004 J. Phys.: Condens. Matter 16 5151

(http://iopscience.iop.org/0953-8984/16/28/033)

INSTITUTE OF PHYSICS PUBLISHING JOURNAL OF PHYSICS: CONDENSED MATTER

J. Phys.: Condens. Matter **16** (2004) 5151–5161 PII: S0953-8984(04)78496-9

Raman scattering study of $NaAl(MoO_4)_2$ crystal under high pressures

W Paraguassu[1], A G Souza Filho[1], M Maczka[2], P T C Freire[1], F E A Melo[1], J Mendes Filho[1] and J Hanuza[2,3]

[1] Departamento de Física, Universidade Federal do Ceará, PO Box 6030, Fortaleza-CE, 60455-970, Brazil
[2] Institute of Low Temperature and Structure Research, Polish Academy of Sciences, PO Box 1410, 50-950 Wrocław 2, Poland
[3] Department of Bioorganic Chemistry, Faculty of Engineering and Economics, University of Economics, 53-345 Wrocław, Poland

E-mail: wp@fisica.ufc.br

Received 26 March 2004
Published 2 July 2004
Online at stacks.iop.org/JPhysCM/16/5151
doi:10.1088/0953-8984/16/28/033

Abstract

The high-pressure Raman spectra of ferroelastic $NaAl(MoO_4)_2$ have been measured at room temperature. The studies indicated that this crystal exhibits two pressure-induced phase transitions at about 1.1 and 3.3 GPa. The first transition is connected with slight rotation of the MoO_4^{-2} tetrahedra with loss of the inversion centre. The second transition is connected with significant distortion of the MoO_4^{2-} tetrahedra and Al^{3+} coordination sphere. By performing the lattice dynamics calculations in the starting phase (monoclinic C_{2h}^6) we have been able to make an assignment of the Raman modes of this material. The deep knowledge of the modes helped us to get fundamental insights into the mechanism driving the structural changes occurring in $NaAl(MoO_4)_2$. The two phase transitions observed in the 0.0–4.2 GPa pressure range are completely reversible.

1. Introduction

$NaAl(MoO_4)_2$ belongs to the group of layered crystals with the general formula $M^IM^{III}(M^{VI}O_4)_2$, where $M^I = Na, K, Rb, Cs$, $M^{III} = Al, Sc, In$ and $M^{VI} = Mo, W$, which have been of considerable scientific interest due to their rich polymorphism [1–4]. The phase transitions in this family of crystals lead to symmetry lowering of the crystal structure to $C_{2h}^6 = C2/c$, $C_{2h}^3 = C2/m$ or $C_i^1 = P1$ [1]. $NaAl(MoO_4)_2$ is ferroelastic at ambient conditions and it is isostructural with $NaFe(MoO_4)_2$, belonging to the $C2/c$ space group (hereafter phase I) [5]. The temperature-dependent study of $NaAl(MoO_4)_2$ in the 93–493 K range showed that the monoclinic structure was stable up to the melting point temperature [6].

The temperature-dependent Raman studies for some layered molybdates and tungstates revealed the presence of unusually narrow stretching modes whose frequency and linewidth were almost temperature independent, not being affected by the several phase transitions found in these compounds [6, 7]. On the other hand, the frequency and linewidth of the broad stretching modes were temperature dependent and strongly affected by the phase transitions. Recent high-pressure studies of trigonal $KSc(MoO_4)_2$ showed that investigation of the relationship between the narrow stretching modes and the tetrahedron configuration gives fundamental insight into the driving mechanism of the structural changes observed in double molybdates [8]. The hydrostatic pressure is the cleaner tool for probing the tetrahedron configuration and their interactions.

In this work we report a high-pressure Raman study of a layered $NaAl(MoO_4)_2$ crystal. The nature of the vibrational modes for the starting monoclinic phase (hereafter phase I) is discussed based on the lattice dynamics calculations. We have observed changes in the Raman spectra at about 1.1 and 3.3 GPa which indicated the onset of two pressure-induced first-order phase transitions. The stable phase between 1.1 and 3.3 GPa is probably C_2 or C_s (hereafter phase II). The stable phase above 3.3 GPa (hereafter phase III) is probably still layered, and the Mo atoms preserve the tetrahedral coordination. The increase of pressure increases the interactions between the MoO_4^{2-} tetrahedral thus leading to significant distortions of these units.

2. Experimental details

The growth of a $NaAl(MoO_4)_2$ single crystal has been described elsewhere [6]. In order to perform the high pressure Raman experiments, the sample was polished, nearly along the face perpendicular to z axis, until the thickness of about 80 μm was reached. A tiny piece with surface area of about 0.225 mm^2 was placed inside the pressure cell.

The pressure-dependent Raman spectra were obtained with a triple-grating spectrometer (Jobin Yvon T64000) equipped with a N_2-cooled charge-coupled device (CCD) detection system. The 514.5 nm line of an argon ion laser was used as excitation. An Olympus microscope lens with a focal distance $f = 20.5$ mm and numeric aperture NA $= 0.35$ was used to focus the laser beam on the sample surface. High-pressure Raman experiments were performed using a diamond anvil cell (DAC from Diacell) with 4:1 methanol:ethanol mixture as transmitting fluid. The pressure calibration was achieved by using the well known pressure shift of the ruby luminescent lines.

3. Results and discussion

In order to understand the general behaviour of $NaAl(MoO_4)_2$ under pressure, it is important to provide a brief discussion of the crystal structure and vibrational properties of the ambient ferroelastic phases. The $NaAl(MoO_4)_2$ structure consists of $[AlMo_2O_8]_{\infty\infty}$ layers separated by the Na^+ cations. The Al^{3+} ions as well as the Na^+ ions are located on the same *bc* plane. It is worth noting that the oxygen atoms O2, O3, and O4 are strongly bonded to the Al^{3+} ions whereas the oxygen atom O1 has only a weak interaction with Al^{3+} ions (see the inset to figure 1). This feature will give rise to a stretching mode with large amplitude along the *c* axis. This mode will be discussed in a forthcoming section. The interaction between the MoO_4^{2-} tetrahedra is weak, and the Mo atoms are purely in a tetrahedral coordination. This is not the case for other members of the family such as $CsBi(MoO_4)_2$ and $CsPr(MoO_4)_2$, for which this interaction is responsible for the unusually large spread in the frequency of the stretching modes [9–12].

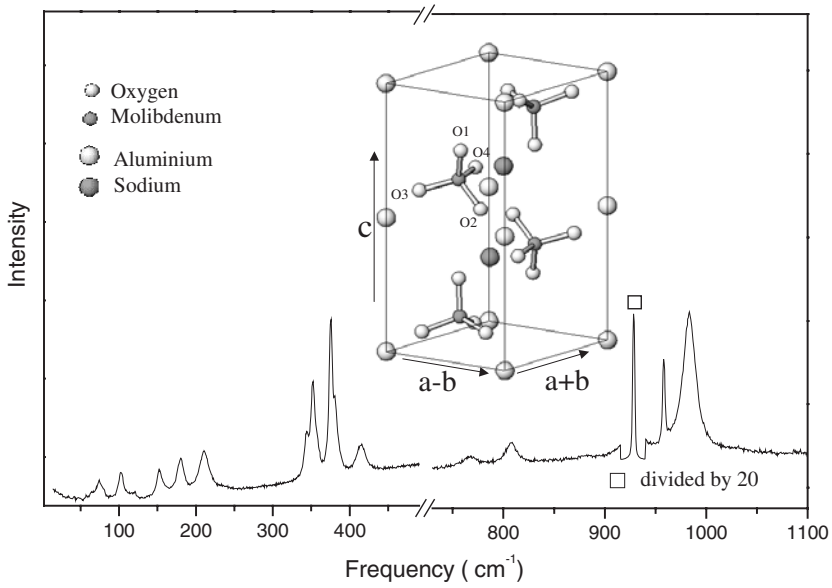

Figure 1. Raman spectrum of $NaAl(MoO_4)_2$ at room temperature and ambient pressure. The intensity of the band marked by a square is divided by 20. The inset of this figure depicts the unit cell of the C_{2h} phase.

The group theory analysis predicts 33 Raman-active modes for the $NaAl(MoO_4)_2$ crystal in the C_{2h}^6 structure. These modes are distributed among the irreducible representations of the factor group C_{2h} as $16A_g + 17B_g$. Of these modes, 18 are internal modes of the MoO_4^{2-} tetrahedra, namely stretching ν_1 ($A_g + B_g$), ν_3 ($3A_g + 3B_g$) and bending ν_2 ($2A_g + 2B_g$) and ν_4 ($3A_g + 3B_g$). The remaining modes stand for translational motions of the Na^+ ions ($A_g + 2B_g$), librations of the MoO_4^{2-} ions ($3A_g + 3B_g$) and translations of the MoO_4^{2-} ions ($3A_g + 3B_g$). The translations of the Al^{3+} ions have A_u and B_u symmetry and they are not Raman active.

In figure 1 we show the Raman spectrum at room temperature and ambient pressure for the $NaAl(MoO_4)_2$ crystal. In order to assign the Raman peaks to the atomic vibrations accordingly, we performed lattice dynamics calculations to predict both frequencies (eigenvalues) and atomic displacements (eigenvectors) for each normal Raman-active mode. Since the $NaAl(MoO_4)_2$ is mostly ionic, we performed the calculations on the basis of a partially ionic model described in the paper by Nozaki *et al* [13]. The atomic positions used in the calculations were taken from x-ray data [5]. The following interatomic potential was used in the lattice dynamics calculations:

$$U_{ij}(r_{ij}) = \frac{z_i z_j e^2}{r_{ij}} + (b_i + b_j)\exp\left[\frac{a_i + a_j - r_{ij}}{b_i + b_j}\right] - \frac{c_i c_j}{r_{ij}^6} + D_{ij}(\exp[-2\beta_{ij}(r_{ij} - r_{ij}^*)] - 2\exp[-\beta_{ij}(r_{ij} - r_{ij}^*)]).$$

This interatomic potential consists of a Coulomb interaction (first term) to model the long-range interactions; a Born–Mayer type repulsive interaction (second term) for accounting the short-range forces; a van der Waals attractive interaction (third term) to model the dipole–dipole interaction and finally the Morse potential contribution (last term) to take into account the covalent bond character. z_i and z_j are the effective charges of ions i and j, respectively, separated by the distance r_{ij}. The parameters (a_i, a_j) and (b_i, b_j) correspond to the ionic radii

Table 1. Parameters used in the lattice dynamic calculations where z are the effective charges of the ions separated by distance r. The parameters a and b correspond to the ionic radii and ionic stiffness, respectively. D_{ij}, β_{ij} and r^*_{ij} are parameters of covalent interaction.

Ion	z (e)	a (Å)	b (Å)	c (kcal$^{1/2}$ Å^3 mol$^{-1/2}$)
Na	0.6	3.22	0.24	300
Al	2.1	2.9	0.24	0
Mo	2.85	2.82	0.23	0
O	−1.05	3.76	0.32	400
Ionic pair	D_{ij} (kcal mol^{-1})	β_{ij} (Å)	r^*_{ij} (Å)	
Mo–O	28.0	2.3	2.0	

and ionic stiffness, respectively. The parameters used in the present calculations are listed in table 1. Since we consider covalency for the Mo–O bond only, D_{ij}, β_{ij} and r^*_{ij} are given for this bond. The parameters were set to values such as shown in table 1 in order to obtain the best agreement between the observed (Raman and infrared (not discussed here) results) and calculated frequencies.

The vibrational frequencies of the observed Raman modes along with their assignments are listed in table 2. The calculated frequencies and atomic displacement vectors for some Raman-active modes of $NaAl(MoO_4)_2$ are shown in figure 2. The atomic displacement vectors corresponding to the A_g mode observed at 928 cm^{-1} involve very large stretching motion of the Mo–O1 bond (see figure 2(b)) which projects into the interlayer. The two stretching modes observed at 983 and 808 cm^{-1} involve large stretching motions of the other three Mo–O bonds (figures 2(a) and (c)). The stretching mode, observed at 765 cm^{-1}, involves mainly motions of the O3 and O4 oxygen atoms (figure 2(d)). This result agrees with previous papers reporting a strong intensity polarization dependence of these modes; i.e., the 928 cm^{-1} mode was observed as a strong mode for the zz geometry and weak for the xx geometry. An opposite behaviour was noticed for the remaining stretching modes [6]. The same behaviour was also observed for other tungstates and molybdates [14, 15].

It has been reported for the $KSc(MoO_4)_2$ crystal that the small linewidth of the 926 cm^{-1} mode can be explained by the fact that the Mo–O1 bonds interact only with the monovalent cation. As a result this mode is characterized by very weak anharmonicity. Weak anharmonicity is further supported by the temperature dependence of both frequency and linewidth observed in this material [6]. Another result of our lattice dynamics calculation is the prediction of a large Davydov splitting for this narrow mode. The previous reports showed that the frequency difference between A_g and B_g components (Davydov splitting) is very small for the majority of modes involving MoO_4^{2-} vibrations and, therefore, these pairs are observed as single lines in the depolarized spectra [6]. However, a few modes of the same origin show large Davydov splitting. These modes have frequency of 958 + 928, 358 + 352 and 157 + 152 cm^{-1}. The remaining modes show no measurable Davydov splitting. This feature is also reproduced by our lattice dynamics calculation. The modes observed in the range of 414–344 cm^{-1} are identified as bending vibrations of the MoO_4^{-2} units (figures 2(e)–(i)). According to the factor group analysis there should be $2B_g + A_g$ translations of Na^+, $3B_g + 3A_g$ translations of MoO_4^{2-} and $3B_g + 3A_g$ librations of MoO_4^{2}. However, the calculations suggest a strong coupling between many modes. The calculated B_g translations of the Na^+ ions have frequencies of 245 and 206 cm^{-1} but they contribute significantly to the 279 cm^{-1} [T′(MoO_4)] and 177 cm^{-1} [T′(MoO_4)] modes. The third calculated B_g translation of the MoO_4^{-2} units has frequency at about 165 cm^{-1}. The calculated B_g modes at 121, 100 and 45 cm^{-1} are nearly pure librations of the MoO_4^{2-} ions.

Table 2. Pressure intercepts ω_0 and pressure coefficients α for ambient-pressure, intermediate and high-pressure phases of the $NaAl(MoO_4)_2$ crystal. ν_1, ν_3, δ, $T'(MoO_4)$, $L(MoO_4)$, $T'(Al^{3+})$ and $T'(Na^+)$ represent, respectively, symmetric stretching, asymmetric stretching, bending, translation and libration of the MoO_4^{2-} ions as well as translation of Al^{3+} and Na^+ ions.

$\omega(P) = \omega_0 + \alpha P$						
Ambient-pressure phase (phase I)		Intermediate phase (phase II)		High-pressure phase (phase III)		
ω_0 (cm^{-1})	α (cm^{-1} GPa^{-1})	ω_0 (cm^{-1})	α (cm^{-1} GPa^{-1})	ω_0 (cm^{-1})	α (cm^{-1} GPa^{-1})	Assignment
982.7	10.4	1003.6	−4.5	977.8	2.2	
		992.0	−4.9	960.7	2.0	ν_3 (MoO_4)
		955.9	3.1			
957.8	2.4	922.1	2.8	930.2	0.4	
		891.6	−0.5	900.0	−2.0	ν_1 (MoO_4)
				858.9	0.9	
				854.6	−0.8	
928.6	−2.5	816.0	2.0	813.2	2.2	
807.5	6.6	808.4	0.0	807.1	−0.7	
764.5	8.8	779.4	0.5	752.3	2.0	ν_3 (MoO_4)
		769.8	−0.6	699.3	−1.1	
414.1	4.3	423.9	14.7	525.3	2.1	
381.3	0.5	406.8	13.8	473.9	5.2	
375.0	0.9	388.7	5.7	462.0	5.4	
357.6	2.6	373.3	7.8	442.9	5.0	
351.8	1.9	372.6	3.5	433.0	4.9	
343.6	−0.7	351.4	7.6	400.3	2.8	δ (MoO_4)
		345.1	6.6	373.5	3.3	
		338.4	4.3	361.9	1.8	
		334.2	9.5	345.6	2.5	
		323.6	6.5	337.0	1.3	
				327.8	0.4	
				313.4	1.8	
211.1	−2.9	268.0	10.4	300.0	1.6	
179.5	4.8	263.9	6.5	286.0	−0.6	
157.4	7.2	222.7	12.6	284.9	0.9	
152.1	0.7	197.1	12.4	258.9	1.9	
		169.5	13.0	228.2	2.7	$T'(MoO_4)$ coupled
		169.4	3.9	221.9	6.1	to $T'(Na^+)$ and
		149.4	1.5	209.3	3.8	$T'(Al^{3+})$
		144.6	5.5	197.3	1.6	
				191.9	4.7	
				188.7	2.4	
		114.8	7.4	177.5	2.1	
118.4	4.2	94.8	8.5	160.9	1.5	
103.7	0.7	91.4	7.6	151.3	1.4	
101.9	−7.2	89.1	−1.2	136.1	2.7	
78.4	1.7	84.1	5.4	128.1	2.0	
74.4	−2.5	77.4	4.4	111.1	3.1	$L'(MoO_4)$ coupled
65.1	−5.6	67.6	4.4	106.2	2.2	to $T'(MoO_4)$
		47.4	4.0	92.8	2.9	
		45.7	10.1	78.3	3.8	
		37.4	5.3	73.2	0.9	
				58.1	0.3	

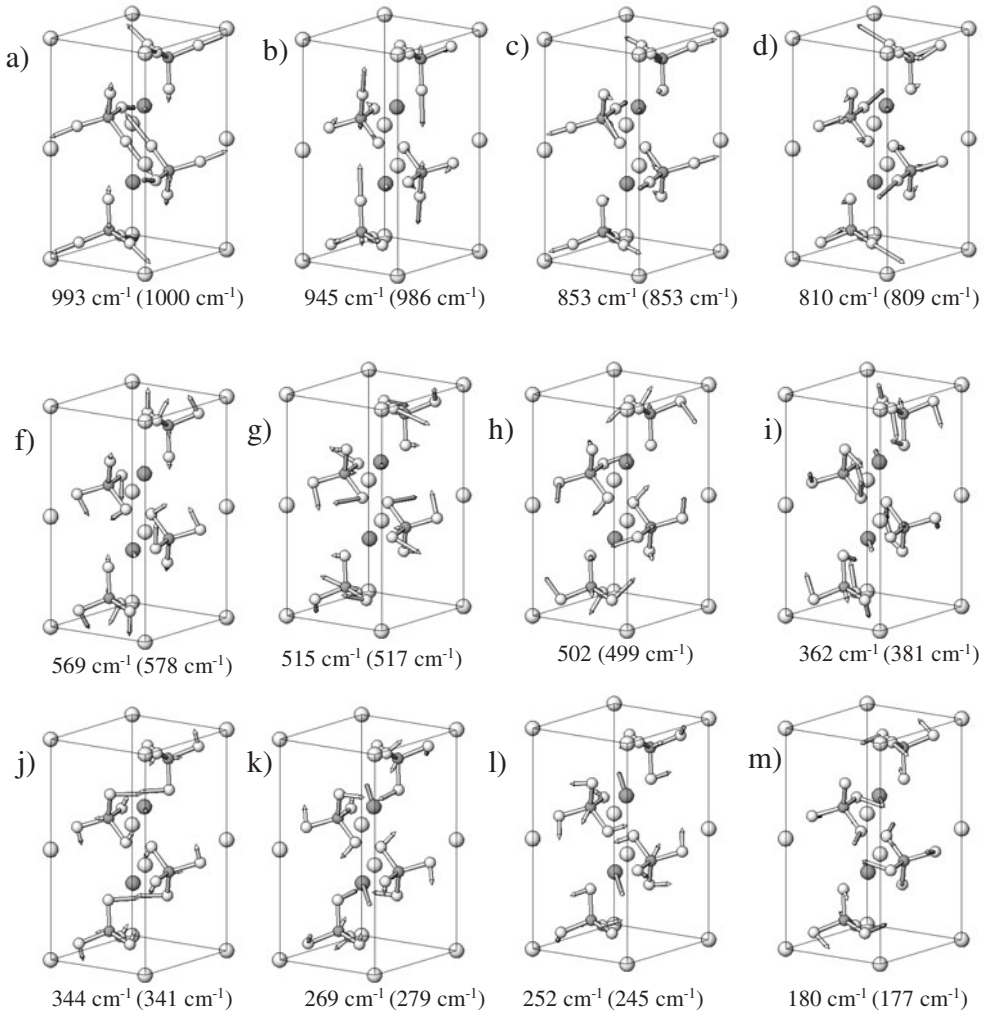

Figure 2. Calculated A_g (B_g) mode frequencies and related atomic displacement for some Raman-active normal modes of $NaAl(MoO_4)_2$ in the C_{2h} structure.

In the same way the A_g modes at 269 and 252 cm^{-1} are coupled modes involving a very large contribution of Na^+ vibration and a smaller contribution of MoO_4^{2-} translations. Previous reports based only on experimental data suggest that the Raman-active translational modes of Na^+ ions were located at lower frequencies (in the range between 120 and 130 cm^{-1}), so this result must be revised [6]. The calculated modes at 180, 152, 132, 98 and 81 cm^{-1} are modes with mixed character involving translations plus librations of the MoO_4^{2-} units. The lattice dynamics calculations helped us to make a definite assignment of the Na^+ translations.

At this point it is worth analysing the relationship between the monoclinic ambient phase of the $NaAl(MoO_4)_2$ crystal and the trigonal phase found in related materials. The observed bands at 808 and 765 cm^{-1} correspond to the E_g stretching mode and the bands above 900 cm^{-1} to the A_{1g} stretching modes of the trigonal phase. The observed bands in the range of 344–381 cm^{-1} correspond to two E_g bending modes and the band at 414 cm^{-1} to the A_{1g} bending mode of the trigonal phase. The bands in the range of 152–211 cm^{-1} correspond most probably to the E_g

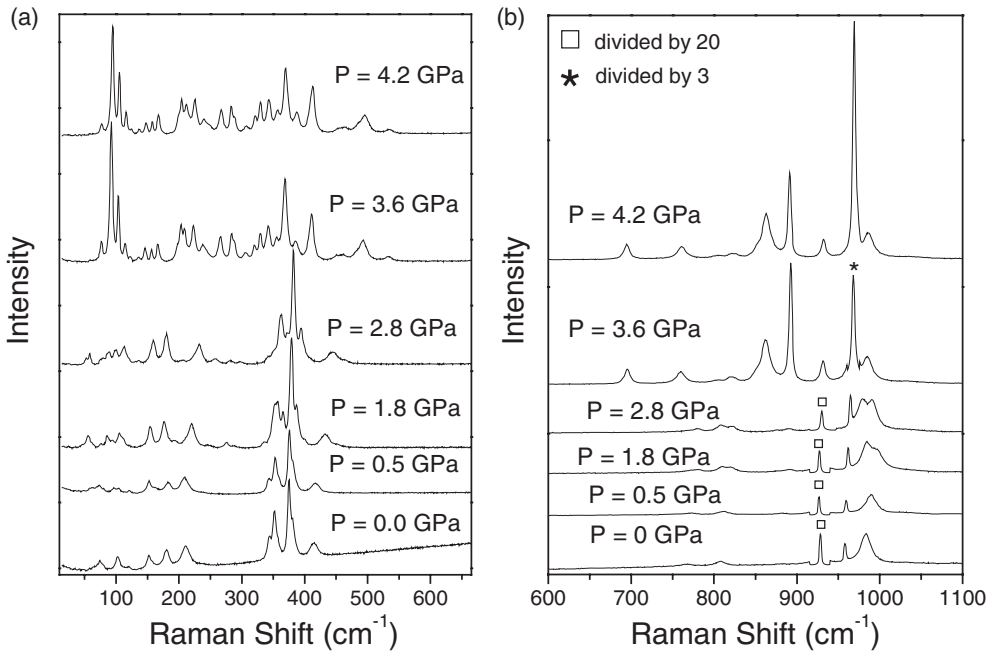

Figure 3. Raman spectra of $NaAl(MoO_4)_2$ recorded at different pressures during compression experiments. The left-hand (right-hand) panel shows the low- (high-) frequency regions of the spectra. The lines in the spectra marked by a square and asterisk are divided by a factor of 20 and 3, respectively. The scattering polarization is close to zz.

and A_{1g} $T'(MoO_4)$ modes in the trigonal phase and the bands at 74 and 78 cm^{-1} (the higher-frequency mode is clearly visible at higher pressures) correspond to the librational mode of E_g symmetry in the trigonal phase. The 104 and 65 cm^{-1} modes can be most probably attributed to the zone boundary modes in the trigonal phase which are folded into the BZ centre as a result of the phase transition. These modes are most probably soft modes since they show frequency decrease with increasing pressure. The remaining mode observed at 118 cm^{-1} originates most probably from the Raman-inactive A_{2g} librational mode in the trigonal phase.

Now that we get a clear picture of the vibrational properties of $NaAl(MoO_4)_2$ at ambient conditions through the lattice dynamics analysis we move to discuss the effects of hydrostatic pressure on the structural and vibrational properties of this compound. We have performed depolarized Raman experiments on an $NaAl(MoO_4)_2$ crystal at room temperature, changing the pressure from 0.0 to 4.2 GPa. In this pressure range we could observe strong modifications in the Raman spectra (see figure 3). The remarkable changes occur at about 1.1 and 3.3 GPa and they can be followed in detail by analysing the frequency (ω) versus pressure (P) plot shown in figure 4. We can note that the pressure dependence of phase I is strong for the stretching modes at 983, 764 and 808 cm^{-1} and weak for the narrow peaks at 928 and 958 cm^{-1} (figure 4(c)). This experimental result confirms that the Mo–O1 bond lengths (O1 is not connected to Al^{3+}) do not change with pressure but the Mo–Oi ($i = 2, 3, 4$) bond lengths (where the O are connected to Al) change significantly. Upon increasing pressure we observe that the frequency of the band at 928 cm^{-1} (958 cm^{-1}) decreases (increases) (figure 4(c)). This behaviour can be most probably explained as a result of interaction strengthening among the crystallographically equivalent MoO_4^{2-} tetrahedra. It is known that the magnitude of Davydov splitting is proportional to the interaction level among the units. The application of pressure is expected to increase the

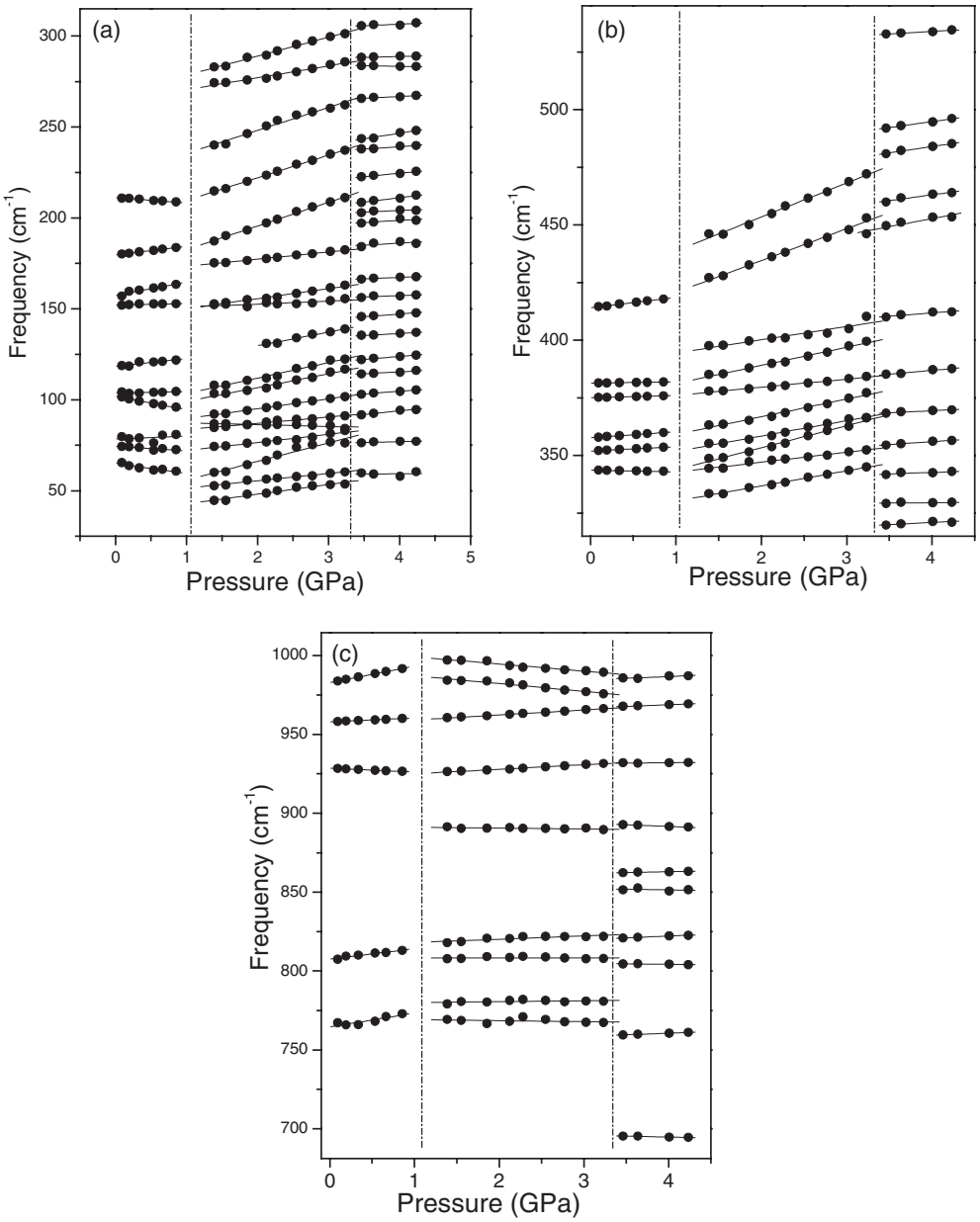

Figure 4. Frequency versus pressure plot for the lattice (a), bending (b) and stretching (c) modes during compression. The solid lines are linear fits of the data to $\omega(P) = \omega_0 + \alpha P$. The vertical dotted lines roughly indicate the pressures at which the transitions take place.

interaction among the MoO_4^{2-} units and consequently should lead to an increase in the splitting. Therefore, the observation of this behaviour for the narrow lines supports our assignment that these two distinct lines come from the Davydov splitting.

At about 1.1 GPa significant changes become evident in the Raman spectra due to a first-order phase transition (see figures 3 and 4). As a result of this phase transition the narrow bands

at 928 and 958 cm^{-1} do not experience either frequency or intensity changes. The remaining bands also show weak changes (small frequency shifts and weak intensity changes). The main change observed in the spectra is related to splitting of several bands. It should be pointed out that most of these additional modes that appear above 1.0 GPa have frequencies close to the IR active modes of the C_{2h} phase [7]. This suggests that as a result of this transition the inversion centre is lost, i.e. the structure is no longer C_{2h} but a symmetry lowering to C_2 or C_s has occurred. Due to this we can argue that the structure changes during the phase transformation were minor, i.e. the phase transition is connected with slight rotations of the MoO_4^{2-} tetrahedra thus leading the AlO_6 octahedron to be distorted in such a way that the inversion centre on Al^{3+} ions has been lost. In this way the four crystallographically equivalent MoO_4^{2-} tetrahedra in the C_{2h} structure form two sets of crystallographically distinct tetrahedra in phase II. This is the reason why we observe the splitting for many modes, including the appearance of a new stretching mode at 890 cm^{-1} (figure 3(b)). Remarkable changes in the mode frequencies are observed below 200 cm^{-1} (lattice mode region). This confirms that the Al–O bonds are most significantly affected by this phase transition whereas the Mo–O bonds practically do not change. A similar argument can be used for Na–O bonds: these bonds are weakly affected by the transition since we have not seen changes for the narrow stretching modes at 928 and 958 cm^{-1}. The pressure dependence of the modes in phase II shows that with increasing of pressure the intensity of a number of weak bands, which were originally IR active in phase I, increases (figure 3(b)). This indicates that during pressure loading AlO_6 octahedra become more distorted and further departures from a centrosymmetric structure occur. We may also notice that some stretching modes (986 and 997 cm^{-1}) have $\frac{\partial \omega}{\partial P} < 0$. This behaviour indicates that increase of pressure strengthens the interaction among MoO_4^{2-} tetrahedra and subsequently leads to a decreasing of some Mo–O bond lengths. However, this change happens only for those oxygen atoms which are connected to Al atoms in the layer. We may say, therefore, that similarly as in the case of $KSc(MoO_4)_2$, the pressure induces a distortion of the AlO_6 octahedron, thus decreasing the distance among the MoO_4^{2-}, which results in increasing the repulsion between oxygen atoms and, consequently, in structural instabilities and the phase transition [8].

At about 3.3 GPa, the $NaAl(MoO_4)_2$ crystal exhibits another first-order phase transition, where the spectra indicated that the material has experienced drastic structural changes. First of all we may say that this transition leads to significant changes in the Mo–O bond lengths (which is largely due to increase of interactions between MoO_4^{2-} units). This is clearly seen in the spectra since the stretching mode region is much broader (695–985 cm^{-1}) than in phase II, thus meaning a much larger distribution of Mo–O bond lengths. Moreover, the bending mode region is also much broader (figure 3(a)). In spite of these changes, the Mo coordination is still tetrahedral. The number of modes did not increase and we could not observe any modes below 60 cm^{-1} which could arise from folding of the zone boundary modes belonging to phase II into the BZ centre. Therefore, it seems that there is no doubling of any lattice parameter (probably the primitive cell still contains only two $NaAl(MoO_4)_2$ formulae). As a result of this transition large changes are also observed for the narrow stretching modes (i.e. frequency shifts and intensity changes). This result shows that Na–O bonds are also strongly affected by this transition. However, some modes are still very narrow (modes at 969 and 891 cm^{-1} have linewidth of 4 cm^{-1}) so this may suggest that in phase III some oxygen atoms still have contact only with Na^+ ions and not with Al^{3+} ions. This means that phase III is still layered with Na^+ ions as spacers but the MoO_4^{2-} tetrahedra are strongly rotated, thus leading to a large distortion of the Al coordination sphere. Such a conclusion is supported by reversibility of the phase transition (figure 5): if the phase were not layered the transition would lead to the breaking of many bonds and then the high-pressure phase would be quenchable. Finally, we

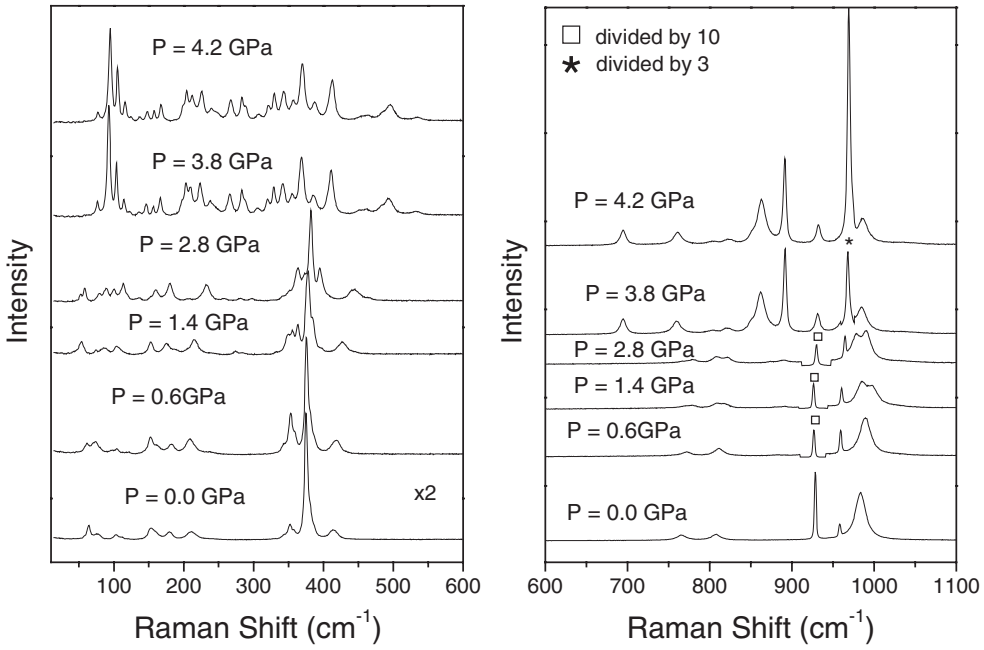

Figure 5. Raman spectra of $NaAl(MoO_4)_2$ recorded at different pressures during decompression experiments. The left-hand (right-hand) panel shows the low- (high-) frequency regions of the spectra. The lines in the spectra marked by a square and asterisk are divided by a factor of 20, 18 or 3 respectively. The spectrum measured at 0.0 GPa is multiplied by a factor of 2. The scattering polarization is close to zz.

can note that many lattice bands in phase III have relatively strong intensity (much stronger than in phase II) thereby further supporting the conclusion that the coordination sphere of Al atoms is strongly distorted in this phase.

4. Conclusions

The present study has provided significant insight into properties of layered molybdates and mechanisms of pressure-induced phase transitions occurring in these crystals. Firstly, it has led to a definite assignment of the vibrational modes of the monoclinic phase (phase I) of the $NaAl(MoO_4)_2$ crystal. Additionally, this study has shown that the unusual negative pressure dependence of some stretching modes can be explained as a result of a significant increase of interactions between the MoO_4^{2-} tetrahedra. This increase gives rise to instability of the structure and a phase transition at 1.1 GPa connected with significant changes of the Al^{3+} coordination sphere due to weak reorientation of MoO_4^{2-} and resulting in loss of the inversion centre during the phase transition to phase II. It is likely that a symmetry lowering effect from C_{2h} to C_2 or C_s has occurred. With further increase of pressure the repulsive forces among the oxygen atoms are so strong that a major reconstruction of the unit cell occurs to release the energy. In this way we have the transition into phase III at 3.3 GPa, which has a completely different Raman spectrum from phases I and II. This transition is related to strong distortion of the MoO_4^{2-} tetrahedra and significant changes in the Al^{3+} coordination sphere. The reversibility of all the transitions suggest that phase III is still layered with Na^+ as spacers.

Acknowledgments

The authors thank Professor Y Morioka from Saitama University (Japan) for allowing us to use his lattice dynamics software. WP and AGSF acknowledge financial support from the Brazilian agencies CNPq and CAPES (PRODOC grant No 22001018), respectively. PTCF acknowledges FUNCAP for grant number 017/96 P&D (Cryogenic DAC). The Brazilian authors acknowledge partial support from Brazilian agencies (FUNCAP, CNPq and FINEP).

References

[1] Otko A I, Nesterenko N M and Povstyanyi L V 1978 *Phys. Status Solidi* a **46** 577
[2] Nesterenko N M, Fomin V I and Zvyagin A I 1979 *Izv. Akad. Nauk. SSSR* **43** 1675
[3] Zapart W 1990 *Phys. Status Solidi* a **118** 447
[4] Zapart M B and Zapart W 1993 *Phase. Transit.* **43** 173
[5] Kolitsch U, Maczka M and Hanuza J 2003 *Acta Crystallogr.* **59** I10
[6] Maczka M, Kojima S and Hanuza J 1999 *J. Raman Spectrosc.* **30** 339
[7] Maczka M, Hanuza J, Lutz E T G and van der Maas J H 1999 *J. Solid State Chem.* **145** 751
[8] Saraiva G D, Maczka M, Freire P T C, Mendes Filho J, Melo F E A, Hanuza J, Morioka Y and Souza Filho A G 2003 *Phys. Rev.* B **67** 224108
[9] Klevtsov P V and Sinaiko V A 1975 *Zh. Neorg. Khim.* **20** 2104 (in Russian)
[10] Paraguassu W *et al* 2004 *Phys. Rev.* B **69** 094111
[11] Fomichev V V and Kondratov O I 1992 *Russ J. Inorg. Chem.* **37** 587
[12] Gnezdilov V P, Eremenko V V, Nesterenko N M and Fomin V I 1990 *Opt. Spektrosk.* **68** 324
[13] Nozaki R, Kondo J N, Hirose C, Domen K, Wada A and Morioka Y 2001 *J. Phys. Chem.* B **105** 7950
[14] Nesterenko N M, Fomin V I, Peschanskii A V and Mitkevich V V 2000 *Ferroelectrics* **239** 101
[15] Maczka M, Hanuza J, Jiang F and Kojima S 2001 *Phys. Rev.* B **63** 144101